THE JOURNAL OF BIOLOGICAL CHEMISTRY Vol. 276, No. 50, Issue of December 14, pp. 47239–47247, 2001
Printed in U.S.A.

Characterization of the *Saccharomyces cerevisiae* Homolog of the Melatonin Rhythm Enzyme Arylalkylamine *N*-Acetyltransferase (EC 2.3.1.87)*

Received for publication, July 30, 2001, and in revised form, September 13, 2001
Published, JBC Papers in Press, September 14, 2001, DOI 10.1074/jbc.M107222200

Surajit Ganguly‡, Padmaja Mummaneni‡, Peter J. Steinbach§, David C. Klein‡¶ and Steven L. Coon‡

From the ‡Section on Neuroendocrinology, Laboratory of Developmental Neurobiology, NICHD, National Institutes of Health, Bethesda, Maryland 20892-4480 and the §Center for Molecular Modeling, Center for Information Technology, National Institutes of Health, Bethesda, Maryland 20892-5626

Arylalkylamine *N*-acetyltransferase (AANAT, serotonin *N*-acetyltransferase, EC 2.3.1.87) plays a unique transduction role in vertebrate physiology by converting information about day and night into a hormonal signal: melatonin. Only vertebrate members of the AANAT family have been functionally characterized. Here a putative AANAT from *Saccharomyces cerevisiae* (scAANAT) was studied to determine whether it possessed the catalytic activity of the vertebrate enzyme. scAANAT is 47% similar to ovine AANAT, but lacks the regulatory N- and C-terminal flanking regions conserved in all vertebrate AANATs. It was found to have enzyme activity generally typical for AANAT family members, although the substrate preference pattern was somewhat broader, the specific activity was lower, and the pH optimum was higher. Deletion of scAANAT reduced arylalkylamine acetylation by *S. cerevisiae* extracts, indicating that scAANAT contributes significantly to this process. The scAANAT sequence conformed to the three-dimensional structure of ovine AANAT catalytic core; however, an important structural element (loop 1) was found to be shorter and to lack a proline involved in substrate binding. These differences could explain the lower specific activity of scAANAT, because of the importance of loop 1 in catalysis. Data base analysis revealed the presence of putative AANATs in other fungi but not in the nearly complete genomes of *Drosophila melanogaster* or *Caenorhabditis elegans*. These studies indicate that the catalytic and kinetic characteristics of fungal and vertebrate enzymes can be considered to be generally similar, although some differences exist that appear to be linked to changes in one structural element. Perhaps the most striking difference is that fungal AANATs lack the regulatory domains of the vertebrate enzyme, which appear to be essential for the regulatory role the enzyme plays in photochemical transduction.

The arylalkylamine *N*-acetyltransferase (serotonin *N*-acetyltransferase, AANAT,[1] EC 2.3.1.87) family is part of the motif A/B or GNAT acetyltransferase superfamily, which includes over 250 members (1–3). This superfamily is represented in all phyla, and each family selectively acetylates a substrate group; substrates range in size from proteins to aminoglycosides, diamines, and small amines. The AANAT family exhibits selectivity for arylalkylamines, including serotonin, tryptamine, and phenylethylamine (1). Functional members of the AANAT family have only been identified in vertebrates.

Vertebrate AANAT is closely associated with photochemical transduction, specifically melatonin synthesis (serotonin → *N*-acetylserotonin → melatonin). It is expressed at significant levels in the two tissues in which melatonin is synthesized, the pineal gland (the source of circulating melatonin) and the retina (where melatonin acts locally). In both tissues, the activity of the enzyme is under complex regulation; changes in AANAT activity control the precise day/night rhythm in melatonin production (reviewed in Ref. 2). Accordingly, vertebrate AANAT occupies a unique position in vertebrate biology as the molecular interface between regulatory mechanisms and melatonin synthesis.

Data base searches reveal that members of the AANAT family occur in fungi, including the budding yeast *Saccharomyces cerevisiae*.[2] The sequence from *S. cerevisiae* (scAANAT; GenBank™ accession no. S49826; Ref. 1) was annotated as a hypothetical protein and is ~26% identical[3] and ~46% similar to vertebrate AANATs. Similarity is limited primarily to the catalytic core of vertebrate AANAT and is highest within motifs A/B, which characterize the GNAT superfamily (1, 4). The presence of AANAT in *S. cerevisiae* is of special interest because, if it had arylalkylamine *N*-acetyltransferase activity, it could participate in the formation of melatonin (5, 6); it could also have a broader function in detoxification of arylalkylamines.

In the study presented here, we found the putative scAANAT

* The costs of publication of this article were defrayed in part by the payment of page charges. This article must therefore be hereby marked "*advertisement*" in accordance with 18 U.S.C. Section 1734 solely to indicate this fact.

¶ To whom correspondence should be addressed: Laboratory of Developmental Neurobiology, 49 Convent Dr., MSC 4480, Bldg. 49, Rm. 6A-82, National Institutes of Health, Bethesda, MD 20892-4480. Tel.: 301-496-6915; Fax: 301-480-3526; E-mail: klein@helix.nih.gov.

[1] The abbreviations used are: AANAT, arylalkylamine *N*-acetyltransferase; GNAT, GCN5-related *N*-acetyltransferase; scAANAT, *S. cerevisiae* arylalkylamine *N*-acetyltransferase; hAANAT, human arylalkylamine *N*-acetyltransferase; oAANAT, ovine arylalkylamine *N*-acetyltransferase; ORF, open reading frame; GST, glutathione *S*-transferase; PAGE, polyacrylamide gel electrophoresis; PCR, polymerase chain reaction; AcCoA, acetyl coenzyme A; TLC, thin layer chromatography; PKA, cAMP-dependent protein kinase; PBS, phosphate-buffered saline.

[2] The existence of a putative AANAT in *S. cerevisiae* was noted by Coon *et al*. (1). More recent data base searches using BLASTP have revealed putative AANATs in other fungi as detailed under "Results."

[3] All statistics referring to percentage of identity or percentage of similarity between sequences are based on the output from BLASTP comparisons. Numbers in parentheses (when given) are numbers of identical or similar residues divided by the length of the homologous region used for the calculations.

to be a functional arylalkylamine *N*-acetyltransferase generally similar to that of vertebrates.

EXPERIMENTAL PROCEDURES

Cloning of scAANAT

The scAANAT ORF was amplified by reverse transcription-PCR from *S. cerevisiae* genomic DNA using primers Y01L (AAA TGG CCT CCT CAA GTA GCA C) and Y02R (TCA GTA CGG TCA AGG ATG TAG G). The resulting fragment was cloned into pGEM-T Easy (Promega, Madison, WI). The ORF was excised with *Eco*RI and subcloned into the *Eco*RI site of the prokaryotic expression vector pGEX-4T-1 (Amersham Pharmacia Biotech), which generates a fusion protein with glutathione *S*-transferase (GST). The resulting clone was designated Y14X. The 9 base pairs immediate to 5′ of the ATG start codon were deleted using the QuikChange mutagenesis kit (Stratagene, La Jolla, CA) to reduce the number of amino acid residues and eliminate stop codon between the GST portion of the expressed protein and the ORF of scAANAT. The integrity of this clone (Y2NAT) was confirmed by automated DNA sequencing (Seqwright, Houston, TX).

Expression of scAANAT Protein

The scAANAT-GST fusion protein (clone Y2NAT) construct was transformed into *Escherichia coli* strain BL21(DE3)pLysS (Novagen, Madison, WI). The cells were grown at 37 °C. After about 4 h ($A_{600} \sim 0.5$), the cells were treated (12–15 h, 24 °C) with 0.2 mM isopropyl-β-D-thiogalactopyranoside (Sigma) to induce protein expression. The cells were then harvested (5000 × *g*; 20 min) and suspended in 2× phosphate-buffered saline, pH 7.4 (PBS), containing 10 mM dithiothreitol (Buffer A) and protease inhibitors (Complete™ protease inhibitor mixture tablets; Roche Molecular Biochemicals). All subsequent steps were carried out at 4 °C unless otherwise stated. The cells were homogenized by sonication, and the homogenate was centrifuged (6000 × *g*; 10 min). The supernatant was mixed with glutathione-Sepharose 4B affinity matrix (Amersham Pharmacia Biotech), pre-equilibrated with Buffer A. The suspension was gently agitated for 2 h and packed into a column. The column was washed with Buffer A (5× column volume) and then with 50 mM Tris-HCl, pH 8.0, buffer containing 10% glycerol (Buffer B; 5× column volume). GST fusion protein was eluted with Buffer B containing 10 mM glutathione; fractions containing scAANAT-GST were pooled and dialyzed (12–16 h; three changes; 100× volume) against Buffer A. The dialyzed sample was treated with 1 unit of thrombin (Roche Molecular Biochemicals)/mg of protein (4 °C; ~6 h) to cleave the fusion protein and then mixed (2 h) with a 3:1 (w/w) suspension of glutathione-Sepharose 4B and benzamidine-Sepharose 4B (Amersham Pharmacia Biotech). The mixture was loaded onto a column, and the flow-through volume containing the enzyme activity was collected and concentrated to obtain highly purified scAANAT, as verified by SDS-PAGE. The thrombin-cleaved free scAANAT is expected to have 6 extra amino acids (GSPEFT-) at the N terminus, based on the intervening DNA sequence between the thrombin cleavage site and the ORF start codon.

Measurement of Protein

Protein was determined by monitoring absorbance at 280 nm and by Bradford's protein dye-binding method (Bio-Rad) using bovine serum albumin as standard.

SDS-PAGE Analysis

The purity of expressed proteins was analyzed by SDS-PAGE using precast 14% polyacrylamide gels (Invitrogen, Carlsbad, CA) in a Tris-glycine buffer system (7). Proteins were stained by GelCode® Blue Stain reagent (Pierce) according to the manufacturer's instructions and were visualized after destaining with deionized water for 1 h.

Yeast Strains

Wild Type—The wild type parental yeast strain used was *S. cerevisiae* AH109 (*MAT**a***, *trp1–901*, *leu2–3*, *112*, *ura3–52*, *his3–200*, *gal4*, *gal80*, *LYS2*::*gal1*$_{UAS}$-*GAL1*$_{TATA}$-*HIS3*, *GAL2*$_{UAS}$-*GAL2*$_{TATA}$, *ura3*::*MEL1*$_{TATA}$-*lacZ*); the *ade2–101* gene was replaced with *GAL2-ADE2* reporter construct (CLONTECH, Palo Alto, CA). To allow the wild type strain to grow in the same medium as the mutant strain (see below), AH109 cells were transformed with plasmid pGBKT7, which harbors the *trp* gene.

scAANAT Deletion Mutant—The ORF of *scAANAT* was deleted from parental strain AH109 and replaced with a PCR-amplified *TRP1*-selectable marker by homologous recombination (8). *TRP1* was amplified from vector pGBKT7 (CLONTECH) using the following hybrid primers: FdelY (5′-ATT TAT AAT TAG ACA TTT GTA AAG TGC GTT AAA CTA ATG ATC TAG TTG TAT CAG GAG GCC CTT TCG TCT CGC GCG TT-3′) and RdelY (5′-ACG ATT AAA TAA AAA GTT AAA ATG CCC TCC TCA AGT AGC ACG CTA CCG CGG TAT TTC ACA CCG CAT AGA TCG GCA AG-3′). Each primer consisted of two distinct regions; one was homologous to sequence flanking the *scAANAT* ORF, which was followed by a sequence complimentary to the *TRP1*-selectable marker. The latter region of the primers was required for the proper amplification of the marker, and the former region facilitated homologous recombination of the PCR product into the *scAANAT* ORF. To assess the successful replacement of the *scAANAT* gene with the *TRP1* gene, genomic DNA isolated from the wild type AH109 and scAANAT$^{(-)}$ strains was subjected to PCR using primers F-IDY (5′-GTA GCA CCA GTA GTA ATG AT 3′) and R-IDY (5′ TCA GAA TAC TTT TCT CGG AG-3′) that flank *scAANAT* in *S. cerevisiae* chromosome IV (cosmid 8554, GenBank™ accession no. Z46796).

Culture Conditions for Wild Type and Mutant Yeast

Wild type AH109 and mutant scAANAT$^{(-)}$ yeast strains were maintained on agar plates made with SD-Trp Drop Out culture medium (CLONTECH), supplemented with 0.003% adenine (Sigma). For experiments, one or two colonies were cultured overnight in 10 ml of liquid medium at 30 °C. This overnight culture was used (1:100, unless otherwise specified) to inoculate the larger experimental cultures. Experimental treatments commenced when the cultures reached an optical density at 600 nm of 0.5.

Preparation of Yeast Cell Homogenates and Extracts

Homogenates—Cell homogenates were used to assess enzyme activity in wild type and mutant yeast. Cells were harvested (5000 × *g*; 15 min), washed twice with PBS, and finally suspended in one volume of PBS. The cells were lysed by freezing and thawing (two times), followed by sonication (3 pulses; 1 min each with 1-min resting interval on ice). The lysate was centrifuged (5000 × *g*; 15 min), and the cleared homogenate was used for analysis of acetylation activity.

Extracts—Extracts used to study *N*-acetyltransferase substrates were prepared by precipitating the proteins from homogenates (6% perchloric acid (final); 10 min; on ice). The precipitate was removed by centrifugation (6000 × *g*; 10 min), and the pH of the supernatant was adjusted to pH 6.3 with 2 M K_2HPO_4. The resulting precipitate was removed by centrifugation (6000 × *g*; 10 min) to obtain the final extract.

Assay of AANAT Activity

AANAT activity was measured radiochemically as described previously (1, 9). Unless otherwise indicated, each assay contained tryptamine HCl (10 mM) and [^{3}H]AcCoA (0.5 mM; 4 Ci/mol; PerkinElmer Life Sciences). Assays were performed either in 0.1 M sodium phosphate buffer (pH 6.8) or in a 0.1 M Na_2CO_3-$NaHCO_3$ buffer system (pH 8.6) containing bovine serum albumin (20 μg) in a volume of 100 μl (37 °C; 20 min). The [^{3}H]*N*-acetyltryptamine formed was extracted into 1 ml of chloroform; a 0.5-ml sample was dried, and radioactivity was determined. Acetylation of serotonin was studied using a similar procedure in which serotonin and [^{14}C]AcCoA (0.1 mM; 55 Ci/mol; PerkinElmer Life Sciences) were incubated in 0.1 M sodium phosphate buffer, pH 6.8 (37 °C; 20 min), in a total reaction volume of 40 μl. The radiolabeled product was resolved by thin layer chromatography (TLC) on silica-coated aluminum sheets (Whatman no. 4420 222; Maidstone, Kent, United Kingdom) using a chloroform:methanol:acetic acid (93:7:1) solvent system. The region containing [^{14}C]*N*-acetylserotonin was located by UV quenching of the authentic carrier (1), excised, and immersed in 500 μl of ethanol; radioactivity was measured by scintillation counting.

Substrate specificity of scAANAT was surveyed by incubating the purified recombinant protein with selected amines (1 mM) and [^{14}C]AcCoA (0.1 mM; 55 Ci/mol; PerkinElmer Life Sciences) in 0.1 M phosphate buffer, pH 6.8 (37 °C; 30 min) in a final reaction volume of 40 μl. The reaction was stopped by adding 10 μl of ethanol (20% final) containing authentic acetylated product. Acetylated products were separated from their respective parent amines using TLC as described above for serotonin. The solvent system used was chloroform:methanol:acetic acid (93:7:1), except for *p*-aminobenzoic acid (chloroform:methanol:acetic acid, 80:20:1) and γ-aminobutyric acid (ethyl acetate:acetic acid:butanol:water, 1:1:1:1). Radioactivity on the TLC sheet was observed using a PhosphorImager (Molecular Dynamics, Sunnyvale, CA) to confirm that there was a single acetylated product in all cases; the position of the radiolabeled product was determined by ultraviolet quenching of

the authentic carrier (1). The gel containing the authentic standard was identified, and radioactivity was determined as described above.

Kinetic analysis of selected substrates was done using the assay method described above for tryptamine, but with the amine substrate of interest at the indicated concentrations.

Materials

The chemicals used (sources) follow: 5-methoxytryptamine, tryptamine hydrochloride, serotonin, phenylethylamine, β-OH-phenylethylamine, mescaline, tyramine, 3-methoxytyramine, glucosamine, sulfamethazine, *p*-aminobenzoic acid, γ-aminobutyric acid, aspartic acid, puromycin, melatonin, *N*-acetyltryptamine, *N*-acetylmescaline, *N*-acetylserotonin, acetyltryptophan, and tryptophan (Sigma); dopamine hydrochloride, 2-methyl-5-hydroxytryptamine, and *N*-acetyldopamine monohydrate (Regis Chemical Co., Chicago, IL); 6-fluorotryptamine, α-methyltryptamine, acetanilide, acetylphenetidine, and aniline (Aldrich); and *p*-phenetidine citrate (City Chemical Co., New York, NY). The following were synthesized: *N*-acetylsulfamethazine, *N*-acetyl-α-methyltryptamine, *N*-acetylphenylethylamine, *N*-acetyl-3-methoxytryptamine, *N*-acetylpuromycin, and *N*-acetyl-6-fluorotryptamine (1, 10).

The bisubstrate inhibitor CoA-S-*N*-acetyltryptamine (11) was obtained from Research Biochemicals International (Natick, MA) through the National Institute of Mental Health's Drug Synthesis Program. It is an analog of the presumed reaction intermediate of AANAT and acts by occupying both the AcCoA and arylalkylamine binding pockets in the catalytic domain of oAANAT; CoA-S-*N*-acetyltryptamine very weakly inhibits arylamine *N*-acetyltransferase (11, 12).

Data Base Searches

The data bases searched included nonredundant protein and nucleotide sequence data bases at the National Center for Biotechnology Information (National Institutes of Health, Bethesda, MD). Searches were done using the gapped BLASTP, tBLASTn, and iterative Psi-BLAST programs (13). Sequences identified as putative AANATs were systematically used as query sequences to determine whether they were homologous to known sequences.

Sequence Analysis and Molecular Modeling

A multiple sequence alignment was constructed using the ClustalW program (14). A homology model of scAANAT was built based on the crystal structure of ovine AANAT (oAANAT) with the bisubstrate analogue CoA-S-*N*-acetyltryptamine bound (Protein Data Bank code 1cjw). The two sequences were aligned according to the multiple sequence alignment given in Fig. 4. The SegMod algorithm (15) of the program GeneMine was used to generate the coordinates of scAANAT. Subsequent analysis of the model was performed using the CHARMM program (16). The coordinates of the 261 water molecules in the sheep structure resolved by x-ray crystallography were simply copied into the model, and all protein and water hydrogen atoms were placed using the CHARMM 22 parameter set (17) and the "hbuild" procedure (18). The bisubstrate inhibitor coordinates were then copied into the model. The remaining energetic optimization of the model protein, inhibitor, and waters was performed using the Merck molecular force field (19–23). Following placement of the inhibitor hydrogen atoms, two energy minimizations were performed to allow modest rearrangement of the binding pocket. Electrostatics and van der Waals interactions were shifted to zero at 12 angstroms, and a distance-dependent dielectric ($\epsilon = r$) was used. Because the homology model was made in the absence of the inhibitor, this optimization was performed to alleviate steric clashes without modifying the structure significantly. Protein α carbons were harmonically restrained using a force constant of 100 kcal/mol/Δ^2 in the first energy minimization and 20 kcal/mol/Δ^2 in the second. Each minimization consisted of 25 steps of steepest descents optimization, followed by 1000 steps of adopted-basis Newton Raphson optimization. The resulting structure is illustrated in Fig. 5, using the programs Molscript (24) and Raster3D (25). The model of the yeast protein generated includes 174 residues (Ser-6 to Asp-179) because the template structure of oAANAT includes coordinates only for residues in the range His-30 to Leu-195.

RESULTS

Expression of Hypothetical scAANAT—The hypothetical scAANAT was expressed as a GST fusion protein and purified as described under "Experimental Procedures." The yield from 1 liter of bacterial culture was 3.5 mg of GST-free scAANAT protein. The resulting protein preparation was >95% pure, as indicated by Coomassie Blue staining of the SDS-PAGE gel, which revealed a single major band of protein (Fig. 1). The apparent molecular mass of the band was ~24 kDa (Fig. 1), which is consistent with the predicted mass of 22.6 kDa based on the amino acid sequence deduced from the Y2NAT clone (see "Experimental Procedures"). The expressed protein acetylated tryptamine (10 mM; pH 6.8) with a specific activity of 98.9 ± 66.7 pmol/pmol of enzyme/h (mean ± S.E.; $n = 5$ preparations).

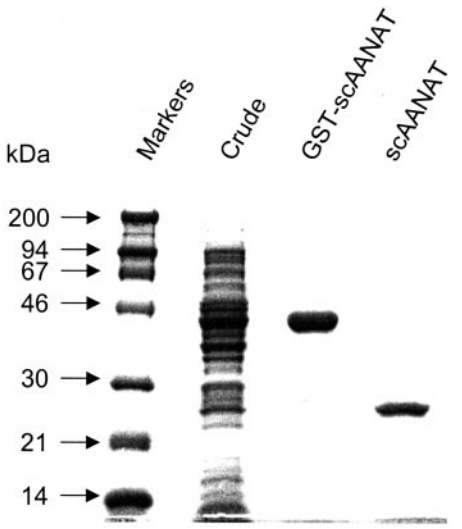

FIG. 1. **Size and purity of scAANAT by SDS-PAGE.** scAANAT was produced in bacteria as a GST-scAANAT fusion protein, and then cleaved with thrombin to release free scAANAT (see "Experimental Procedures"). Samples at each stage of purification were run on a 14% polyacrylamide gel (precast; Invitrogen) in the presence of SDS. Each lane contains 5 μg of protein. The protein bands were visualized on the gel by GelCode® Blue staining as described under "Experimental Procedures." *Crude*, bacterial lysate containing GST-scAANAT; *GST-scAANAT*, combined fractions from glutathione-Sepharose 4B column eluted with glutathione (10 mM); *scAANAT*, free scAANAT from mixed glutathione/benzamidine-Sepharose 4B column following thrombin cleavage. Molecular mass markers are given on the *left*.

Characterization of scAANAT and Comparison with Vertebrate AANAT—The optimum temperature for scAANAT was found to be 42 °C (Fig. 2*A*). The optimum pH for scAANAT activity was pH 8.6 (Fig. 2*B*); the activity at this pH was ~10-fold greater than at pH 6.8, which is the optimum pH for mammalian AANATs (26). scAANAT activity was significantly reduced at pH ~6.0, the optimum pH for trout and pike AANAT-1 and AANAT-2 (27). The specific activity of scAANAT with tryptamine (10 mM) as a substrate at pH 8.6 is ~1/350 that of oAANAT at pH 6.8 (536 pmol/pmol of enzyme/h *versus* ~184,000 pmol/pmol of enzyme/h for scAANAT and oAANAT, respectively).

Substrate specificity of scAANAT was investigated with a selection of amines that have been used to characterize vertebrate AANAT (Table I). A high sensitivity assay using [^{14}C]AcCoA was used to maximize detection of substrates. The pattern of substrate selectivity exhibited by scAANAT was generally similar to that of vertebrate AANATs (Tables I and II). However, it was of interest that dopamine was acetylated by scAANAT at approximately one-third the rate of tryptamine, because oAANAT has been reported not to acetylate this amine (Table III; Ref. 1). Accordingly, although the substrate selectivity patterns of oAANAT and scAANAT are generally similar, that of scAANAT is somewhat broader. The K_m values of the best amine substrates for scAANAT (with AcCoA = 0.5 mM) were 5-methoxytryptamine (K_m ~4.5 mM) < tryptamine ~ serotonin (K_m ~6 mM) < phenylethylamine (K_m ~13 mM) (Ta-

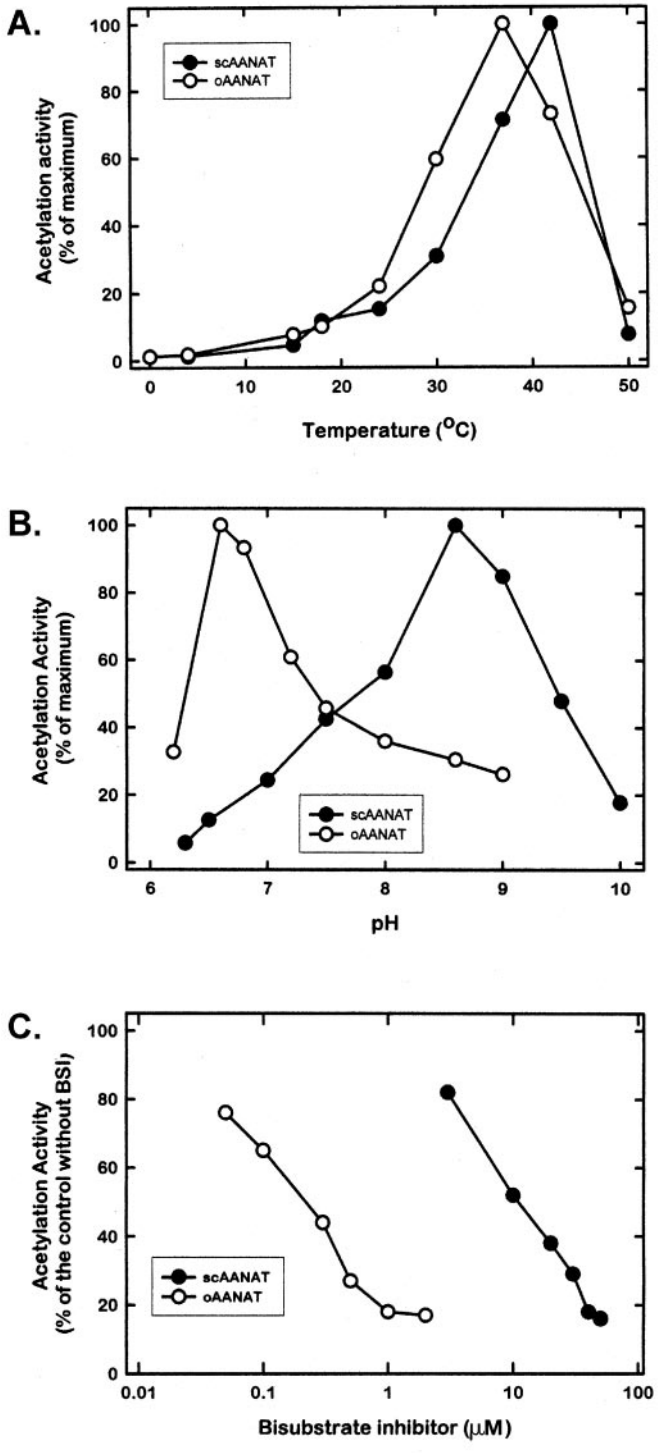

FIG. 2. **Characterization of purified recombinant scAANAT and comparison to recombinant oAANAT.** AANAT activity was measured using a radiometric assay (0.1 M sodium phosphate buffer, pH 6.8; 37 °C; 20 min) in the presence of tryptamine (10 or 1 mM for scAANAT or oAANAT, respectively) and [^{3}H]AcCoA (0.5 mM) as described under "Experimental Procedures" (except as detailed below). *A*, AANAT activity as a function of temperature. Activity was measured at the indicated temperatures. *B*, AANAT activity as a function of pH. scAANAT activity was measured in 0.1 M sodium phosphate buffer (pH range, 6.3–7.6), 0.1 M Tris buffer (pH range, 7.8–8.1), or 0.1 Na_2CO_3-$NaHCO_3$ buffer (pH range, 8.1–10.0); oAANAT was measured with 0.1 M sodium phosphate buffer (pH range, 6.3–9.0). *C*, effect of CoA-S-*N*-acetyltryptamine (a bisubstrate inhibitor) on AANAT activity. The efficacy of inhibition by CoA-S-*N*-acetyltryptamine was assayed at pH 6.8 and 37 °C; the inhibitor was added at the beginning of the assay. The IC_{50} values are ~10 or 0.3 μM for scAANAT and oAANAT, respectively.

TABLE I
Amines tested for acetylation by scAANAT

scAANAT was incubated with the indicated amines (1 mM) and [^{14}C]AcCoA (0.1 mM; 55 Ci/mol). Assays were performed in 0.1 M phosphate buffer, pH 6.8, and were incubated at 37 °C for 30 min. The acetylated products were separated by TLC; the area of the sheet containing the authentic standard was removed and the radioactivity measured. Data were replicated in three independent experiments. Values in parentheses give the relative degree of acetylation as a percent of the 5-methoxytryptamine value. ND, not detected.

Amine (1 mM)	Acetylation by scAANAT
	pmol/pmol enzyme/h
5-Methoxytryptamine	14.5 (100%)
Tryptamine	10.7 (73%)
6-Fluorotryptamine	7.1 (49%)
Mescaline	6.6 (45%)
Phenylethylamine	4.9 (34%)
β-Hydroxyphenylethylamine	3.8 (26%)
Serotonin	3.0 (21%)
Dopamine	2.9 (20%)
Tyramine	2.0 (14%)
Aniline	1.9 (13%)
3-Methoxytyramine	1.8 (13%)
Glucosamine	0.68 (5%)
Sulfamethazine	0.52 (4%)
α-Methyltryptamine	0.33 (2%)
2-Methyl-5-hydroxytryptamine	0.30 (2%)
Phenetidine	0.25 (2%)
γ-Aminobutyric acid	ND
p-Aminobenzoic acid	ND
Puromycin	ND
Tryptophan	ND

ble II). These values, obtained at pH 6.8, are more than 10-fold higher than the reported K_m values of hAANAT and oAANAT; they were essentially unchanged at pH 8.6 (Table II).

Analysis of the K_m for AcCoA measured with 40 mM tryptamine revealed that it was 3–5-fold higher than that of vertebrate AANAT (Table II). The affinity of scAANAT for AcCoA was ~10–20-fold higher than for amine substrates, whereas hAANAT and oAANAT had similar affinities for AcCoA and amines.

scAANAT was inhibited by the bisubstrate inhibitor of vertebrate AANATs, CoA-S-*N*-acetyltryptamine (Fig. 2*C*), consistent with the interpretation that the active site and catalytic mechanism of oAANAT and scAANAT are generally similar. The IC_{50} (~10 μM) for scAANAT is >50-fold higher than that for oAANAT or hAANAT (IC_{50} ~ 0.2 μM) (11); this difference might reflect differences in the binding pockets of scAANAT and mammalian AANATs, as addressed under "Discussion."

Analysis of AANAT Activity in the scAANAT$^{(-)}$ Yeast—The effect of deletion of the *scAANAT* gene on arylalkylamine acetylation was investigated in the *S. cerevisiae* AH109 strain by constructing a line in which the *scAANAT* gene was replaced with a selectable tryptophan (*trp1*) marker gene by homologous recombination with regions flanking the *scAANAT* gene. PCR analysis of wild type and scAANAT$^{(-)}$ mutant genomic DNA confirmed that the amplified products were about 0.73 and 1.4 kilobase pairs, respectively, as expected (Fig. 3).

The scAANAT$^{(-)}$ mutant was characterized by comparing the ability of crude homogenates of wild type AH109 and mutant cells to acetylate various amines. Cells from overnight cultures were harvested and homogenized; aliquots of this crude homogenate were used to measure activity. The ability to acetylate tryptamine and phenylethylamine was reduced 10- and 3-fold, respectively, in scAANAT$^{(-)}$ as compared with scAANAT$^{(+)}$ (Table IV, part A). There was no difference, however, in acetylation of the arylamine, phenetidine, between the two preparations. This indicates that scAANAT is responsible for most of the arylalkylamine *N*-acetylation but not arylamine *N*-acetylation.

TABLE II
Comparison of the K_m values for recombinant scAANAT, hAANAT, and oAANAT

The K_m values for arylalkylamine substrates were determined in 0.1 M phosphate buffer, pH 6.8 (except for the column labeled scAANAT (pH 8.6)), with the AcCoA concentration fixed at 0.5 mM. The K_m values for AcCoA were obtained with tryptamine fixed at 40 mM for scAANAT, 10 mM for hAANAT, and 1 mM for oAANAT. Assays were incubated at 37 °C for 20 min. The K_m values for the amines with oAANAT and hAANAT are from the literature (36), except those for 5-methoxytryptamine, which were determined for this study. Values are means ± S.E. (n = 4).

Substrate	K_m values			
	scAANAT (pH 8.6)	scAANAT (pH 6.8)	hAANAT	oAANAT
		mM		
5-Methoxytryptamine	2.7 ± 0.6	4.5 ± 1.0	0.065 ± 0.028	0.062 ± 0.012
Serotonin	5.1 ± 0.4	6.5 ± 1.2	1.3 ± 0.1	0.31 ± 0.1
Tryptamine	4.7 ± 1.0	5.6 ± 1.5	0.12 ± 0.04	0.20 ± 0.03
Phenylethylamine	10.0 ± 0.7	13.3 ± 1.7	0.31 ± 0.03	3.4 ± 0.3
AcCoA	0.34 ± 0.03	0.51 ± 0.8	0.11 ± 0.02	0.13 ± 0.05

TABLE III
Comparison of acetylation of 5-methoxytryptamine, tryptamine, aniline, and dopamine between scAANAT and oAANAT

In these assays, scAANAT and oAANAT were separately incubated in a reaction of 50 μl containing each amine (10 mM) and [^{3}H]AcCoA (0.5 mM; 4 Ci/mol) in 0.1 M phosphate buffer (pH 6.8). After 20 min at 37 °C, the reactions were stopped using nonradioactive acetylated amines (5 mM) in ethanol (10 μl). For further technical details, see "Experimental Procedures." All values are the mean of two separate experiments done in duplicate; values in parentheses are the relative degree of acetylation compared to 5-methoxytryptamine. ND, not detected.

Substrate (10 mM)	Acetylation activity	
	scAANAT	oAANAT
	pmol/pmol enzyme/h	
5-Methoxytryptamine	104.6 (100%)	163,300 (100%)
Tryptamine	40.3 (39%)	158,700 (97%)
Aniline	4.4 (4%)	690 (0.4%)
Dopamine	11.3 (11%)	ND (0%)

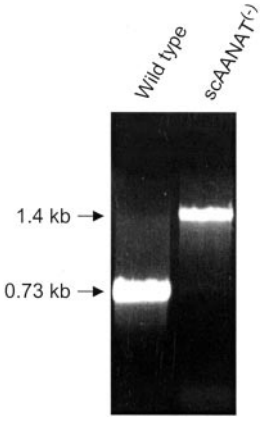

FIG. 3. **Verification of the yeast scAANAT$^{(-)}$ deletion mutant by PCR.** Primers flanking the scAANAT ORF, as described under "Experimental Procedures," were used to amplify genomic DNA from the wild type yeast strain AH109 or the mutant clone, scAANAT$^{(-)}$. The amplified products were separated on an agarose gel and visualized using ethidium bromide. Molecular size markers are given on the *left*. The larger size of the mutant product confirms the replacement of the *scAANAT* gene with the *TRP1*-selectable marker.

Tryptamine acetylation was not inhibited by co-incubation of either wild type or mutant homogenates with phenetidine; conversely, phenetidine acetylation was not inhibited by tryptamine (Table IV, part B). This indicates that tryptamine and phenetidine are acetylated by separate enzymes and that the residual acetylation of tryptamine remaining in scAANAT$^{(-)}$ is not because of cross-reaction with arylamine *N*-acetyltransferase.

Deletion of the *scAANAT* gene also resulted in a reduction in arylalkylamine acetylation *in vivo* compared with the wild type (Table V). The scAANAT$^{(-)}$ mutant accumulated much higher levels of exogenously supplied 5-methoxytryptamine than the wild type, consistent with the interpretation of substantially less acetylation by the mutant. The results were similar whether cells were incubated with 5-methoxytryptamine for either 2 or 18 h.

Sequence Analysis and Molecular Modeling—scAANAT exhibits 26% (41/154) identity and 47% (74/154) similarity with oAANAT (Fig. 4). The parts of the scAANAT sequence that are most similar to the vertebrate AANATs are found in the catalytic core, specifically in motif B and in regions D/c-1 and D/c-2. In addition, some specific residues are conserved that are known to be critical for oAANAT binding and catalysis (28).

One critical difference between scAANAT and the vertebrate AANATs is that scAANAT lacks the N-terminal regulatory region up to the PKA site. It is intriguing, however, that scAANAT contains the sequence Thr-Leu-Pro in almost the exact position as in the vertebrate AANATs; this encompasses oAANAT residue Thr-31, which is part of the PKA/14-3-3 binding site that is important for cAMP regulation of AANAT activity and stability in vertebrates (29, 30). The C-terminal PKA site of vertebrates is also not present in scAANAT.

There is a three-residue gap in scAANAT at the turn of a highly mobile element (loop 1) that forms part of the binding pocket for the arylalkylamine substrate (28). This gap occurs where Pro-64 of oAANAT forms part of the aromatic binding sandwich.

The molecular model of scAANAT included the 174 amino acids that correspond to the portion of oAANAT for which three-dimensional structure is available (Fig. 5*A*). Relative to oAANAT, 43 of the 174 amino acids (25%) are conserved.

Conservation within the AcCoA binding domain revealed that residues that define much of the AcCoA binding pocket in oAANAT (Leu-139, Leu-140, Tyr-143, Leu-164, Pro-166, Phe-167, Tyr-168, and Arg-170) are identical in scAANAT (Leu-123, Leu-124, Tyr-127, Leu-148, Pro-150, Phe-151, Tyr-152, and Arg-154). Tyr-168 of oAANAT has been shown by mutational analysis to be absolutely critical for enzymatic activity (28). The current molecular model also implicates the involvement of oAANAT Arg-170 (scAANAT residue Arg-154) in forming an important salt bridge with the 3′ phosphate of AcCoA. In addition to the important conserved residues, many of the H bonds between enzyme and inhibitor identified by Hickman (28) have counterparts in the model despite differences in sequence. These modest differences observed in the modeled pocket are consistent with the K_m values differing by a factor of 3 (Table II).

The binding pocket for the arylalkylamine substrates is only partly conserved between scAANAT and oAANAT (Fig. 5*B*). Of the three aromatic residues identified by Hickman *et al.* (28) as contributing to the hydrophobic arylalkylamine binding pocket (oAANAT residues Phe-56, Pro-64, and Phe-188), two are identical in scAANAT (Phe-33 and Phe-172). The third residue,

TABLE IV

Comparison of acetylation activity in the cell homogenates of wild type (AH109) and mutant scAANAT$^{(-)}$ yeast strains using exogenous substrates

Homogenates were incubated (20 min, 37 °C) with the indicated amines and [^{3}H]AcCoA as described under "Experimental Procedures." Reactions where the products were finally extracted with chloroform were performed in a 100-μl volume; those reactions to be separated by TLC were done in 20 μl. All values are the mean of two separate experiments done in duplicate. A, scAANAT$^{(-)}$ exhibits reduced arylalkylamine acetylation. At the end of the assay acetyltryptamine, acetylphenylethylamine and acetylphenetidine were extracted into chloroform for counting; acetyldopamine was separated using TLC prior to counting. B, phenetidine does not compete with tryptamine for acetylation. Tryptamine and phenetidine were added either singly or simultaneously. Acetylated products were separated by TLC, and the radioactivity was counted.

A. Substrate	Acetylation activity	
	Wild type	scAANAT$^{(-)}$
	nmol/μg protein/h	
Tryptamine (10 mM)	0.51	0.04 (8%)[a]
Phenylethylamine (10 mM)	1.52	0.50 (30%)
Phenetidine (1 mM)	0.34	0.30 (90%)

B. Substrate	Acetylation activity	
	Wild type	scAANAT$^{(-)}$
	nmol/μg protein/h	
Tryptamine (10 mM)	0.56	0.07
Phenetidine (1 mM)	0.26	0.28
Tryptamine (10 mM)	0.48 (*N*-AcT; 86%)[b]	0.06 (*N*-AcT; 86%)
plus phenetidine (1 mM)	plus 0.23 (*N*-AcP; 88%)	plus 0.25 (*N*-AcP; 89%)

[a] Numbers in parentheses are percentage of wild type values.

[b] Numbers in parentheses are the amount acetyltryptamine (*N*-AcT) and acetylphenetidine (*N*-AcP) produced when tryptamine and phenetidine were added together as a percentage of the amount produced when they were added separately.

TABLE V

The mutant scAANAT$^{(-)}$ has a reduced ability to acetylate arylalkylamines in vivo

Wild type AH109 or mutant scAANAT$^{(-)}$ yeast from overnight cultures were diluted 1:10 into fresh medium. When the cells reached A_{600} ~ 0.5, 5-methoxytryptamine was added to a final concentration of 5 mM and the cells were cultured for another 2 h (A_{600} ~ 1.0) or 18 h (A_{600} ~ 1.7). Cell extracts were prepared as described under "Experimental Procedures." To measure the unutilized 5-methoxytryptamine in the yeast cells, the extracts (10 μl) were incubated separately with oAANAT (1 μg) and [^{14}C]AcCoA (0.2 mM; 53 Ci/mol; Moravek, Brea, CA) in 0.1 M phosphate buffer, pH 6.8, in a final volume of 25 μl. After 30 min, the reaction was stopped with 5 μl of ethanol containing melatonin as an authentic carrier; 30 μl was spotted on a TLC plate and run as described under "Experimental Procedures." The amount of [^{14}C]melatonin formed was determined after extracting it from the TLC plate and was used as a measure of the amount of 5-methoxytryptamine that remained in the cells.

Incubation time	5-Methoxytryptamine remaining in cells	
	Wild type	scAANAT$^{(-)}$
h	*pmol/mg protein*	
2	67.3	156.8 (2.3-fold)[a]
18	100.0	240.8 (2.4-fold)

[a] Numbers in parentheses are the -fold increase over wild type values.

Pro-64, which along with Phe-188 "sandwiches" the indole ring of the substrate, is missing from loop 1 of scAANAT.

Comparison of the oAANAT structure and the derived scAANAT model reveals a conserved element that is not immediately evident from multiple sequence alignments. This is a juxtaposition of three groups of residues, distant in the sequence, that form a "column" of amino acids extending from the core of the molecule to the surface. It extends from His-106 (oAANAT His-122 in strand β5), across strand β4 including Ile-74 and Gly-75, to Cys-51, Pro-52, Glu-53, and Leu-54 in helix α2 at the protein exterior (oAANAT residues Ile-95, Gly-96, Cys-77, Pro-78, Glu-79, and Leu-80, respectively). In addition, there is probable interaction between this column and conserved residues in the core of the molecule. Specifically, Leu-123, Leu-124, Tyr-127, and Gln-134 (oAANAT residues Leu-139, Leu-140, Tyr-143, and Gln-150, respectively) form much of the interior face of helix α4, which is linked to the column described above, in that Tyr-127 and Gln-134 of this helix pack against Gly-75 and Glu-53 of the column.

Another association of interest observed in the model is that a pair of highly conserved residues, Glu-64 and Gly-65 (oAANAT residues Glu-87 and Gly-88), occurs in proximity to the conserved Thr-Leu-Pro sequence at the N terminus of the molecule. As mentioned above, this sequence is part of the oAANAT 14-3-3 binding sequence (Arg-Arg-His-Thr-Leu-Pro).

Data Base Searches—Data base searches revealed two additional fungal AANATs (Fig. 4), one from *Botrytis cinerea* (EMBL accession nos. AL111435 and AL111941)[4] and the other from *Schizosaccharomyces pombe* (GenBank™ accession no. T39187). The *B. cinerea* sequence is 33% (71/214) identical and 47% (102/214) similar to scAANAT, and 26% (21/79) identical and 50% (40/79) similar to oAANAT; the *S. pombe* sequence is 32% (57/174) and 51% (91/174) identical, and 29% (36/122) and 50% (62/122) similar to scAANAT and oAANAT, respectively. The areas of highest similarity to scAANAT are those regions (C/c-1, D/c-1, and D/c-2) that are also highly conserved among vertebrate sequences.

Using BLASTP, scAANAT matches the vertebrate AANATs with expected values ranging down to $E = 2 \times 10^{-7}$, with only other putative fungal AANATs or vertebrate AANATs having expected values below $E = 0.001$. The putative AANAT from *S. pombe* seems to be a better fit to vertebrate AANATs, having matches to the vertebrate AANATs with expected values ranging from $E = 7 \times 10^{-11}$ to 7×10^{-4}. No other members of the GNAT superfamily (including histone *N*-acetyltransferases, aminoglycoside *N*-acetyltransferases, etc.) had expected value scores below $E = 0.1$ when compared with any of the putative fungal AANATs. This indicates that these fungal sequences are unlikely to be orthologs of any vertebrate genes other than those for AANAT.

Apparent orthologs of any fungal or vertebrate AANATs were not found in the essentially complete genomes of *Drosophila melanogaster* and *Caenorhabditis elegans*. It is worth noting that two *N*-acetyltransferases capable of acetylating arylalkyl-

[4] When the data bases were searched using tBLASTn with *S. cerevisiae* as the query, two cDNA sequences from *Botrytis cinerea* were returned (EMBL nos. AL111435.1 and AL111941.1). The nucleotide sequence of the two clones were >99% identical, and the translated open reading frames overlapped for most of their length, with one containing the N terminus and the other the C terminus of the nearly identical peptides. A consensus peptide sequence was generated and used for the multiple sequence alignment.

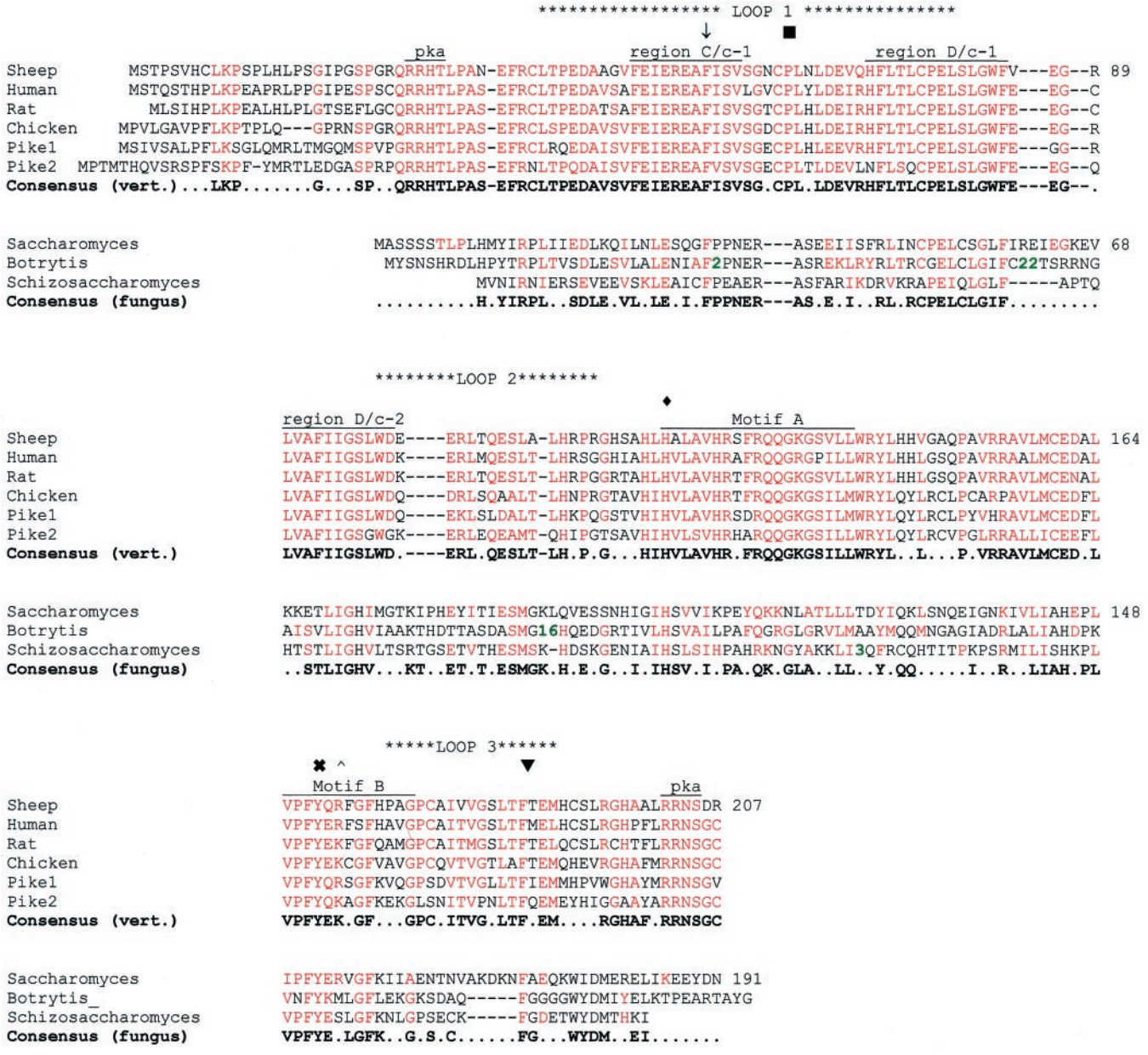

FIG. 4. **Multiple sequence alignment of vertebrate and putative fungal AANATs.** Sequences have been aligned using ClustalW. Consensus sequences for each phylum are shown in *bold*. Residues in *red* are identical or similar to the vertebrate consensus. The data base sequence numbers are as follows (numbers are GenBank accession numbers unless otherwise noted): human (U40346), sheep (U29663), rat (S68435), chicken (U46502), pike 1 (AANAT-1; AF034081), pike 2 (AANAT-2; AF034082), *Saccharomyces* (S49826), *Botrytis* (EMBL AL111435 and AL111941; see Footnote 4), *Schizosaccharomyces* (T39187). -, inserted space; .., no consensus; *bold green numbers*, number of residues removed to maintain optimized alignment; ■, Pro-64 (oAANAT) part of binding sandwich; ▼, Phe-188 (oAANAT) part of binding sandwich; ↓, Phe-56 (oAANAT) part of binding pocket; ^, Arg-170 (oAANAT) part of AcCoA binding pocket; ×, Tyr-168 (oAANAT) in catalytic site; ♦, His-122 (oAANAT) in catalytic site. Regions C/c-1, D/c-1, and D/c-2 are highly conserved in vertebrates as discussed in Ref. 35.

amines have been cloned from *D. melanogaster* (Refs. 31 (GenBank™ accession no. Y07964) and 32 (GenBank™ accession no. CG9486)). Although these genes are members of the GNAT superfamily, they cannot be placed in the AANAT family because they are no more similar to any member of this family than they are to any other member of the GNAT superfamily. These *D. melanogaster* genes have no homolog in fungi or vertebrates based on sequence analysis, although putative orthologs can be identified in *C. elegans* (data not shown). The *D. melanogaster* enzymes acetylate dopamine as a preferred substrate (31, 32).

DISCUSSION

The initial finding of a putative AANAT homolog in yeast (1) raised the question of the function of this protein. The results presented here establish this homolog to be an active arylalkylamine *N*-acetyltransferase with a pattern of substrate selectivity similar to that of vertebrate AANAT. Further evidence of similarity is provided by the observation that the AANAT inhibitor CoA-S-*N*-acetyltryptamine inhibited scAANAT. These observations indicate that a high level of conservation of function is exhibited within the AANAT family, although sequence conservation is relatively modest (47% similarity), emphasizing that functions within protein families can be highly conserved through the course of evolution.

The evidence that the characteristic action of AANAT, acetylation of arylalkylamines, was established early in evolution raises the issue of the physiological function of scAANAT. It is clear that AANAT is an integral component of the melatonin synthesis machinery in vertebrates and that it has no other

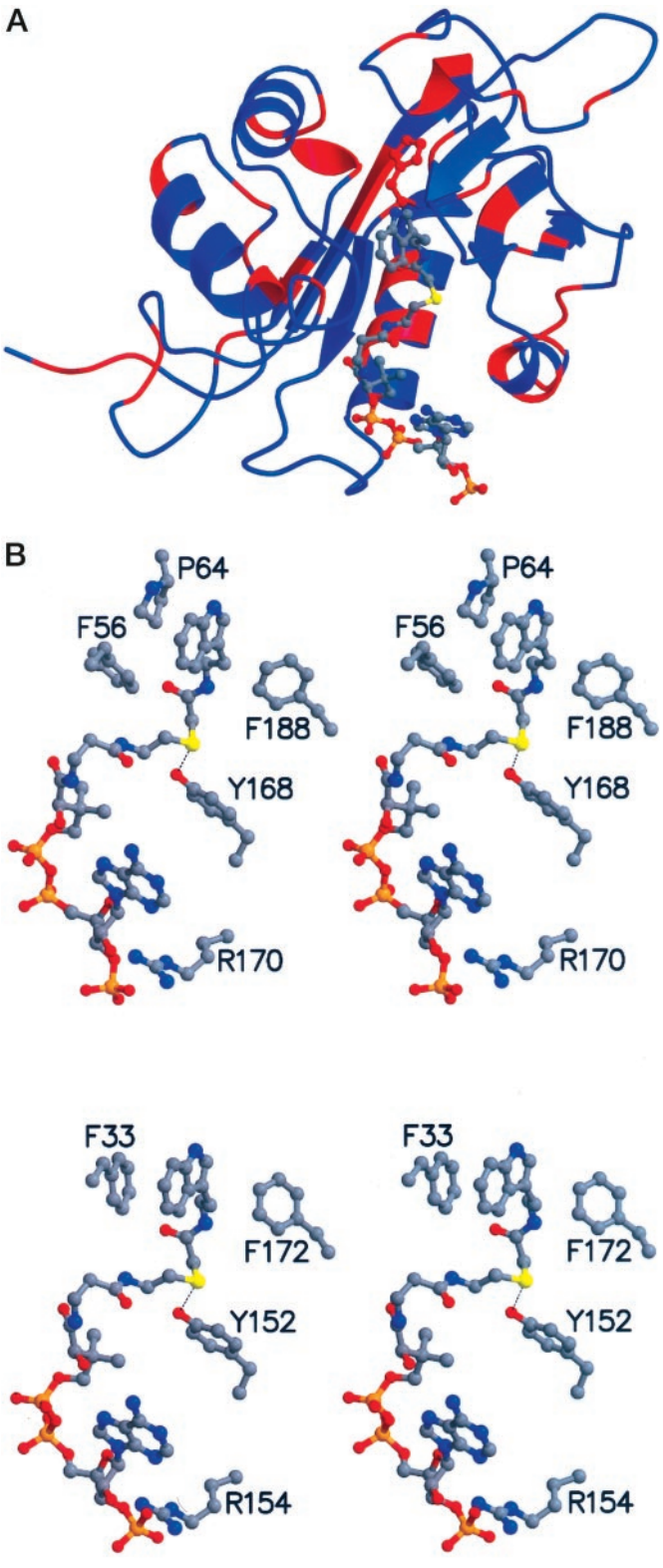

FIG. 5. **Molecular model of scAANAT based on the known crystal structure of oAANAT.** *A*, ribbon structure of the 174 amino acids of scAANAT included in the model. Residues identical to oAANAT are colored *red*. The bisubstrate inhibitor, CoA-S-*N*-acetyltryptamine, and His-106 are shown as a ball-and-stick. The conserved "column" of residues is the adjacent patch of *red* residues receding away from the reader and to the *left* from His-106. *B*, stereoviews (wall-eyed) of the binding pocket of oAANAT (*top*) and scAANAT (*bottom*). The entire bisubstrate inhibitor is displayed along with the side chains of selected conserved residues involved in binding. The residues shown for oAANAT are known to be involved in binding based on the crystal structure; the residues shown for scAANAT are homologous to the residues shown for oAANAT, based on the alignment in Fig. 4.

apparent function. This role reflects two factors; one is the inherent substrate specificity of AANAT, and the second is the setting in which the enzyme is expressed. AANAT is found at significant levels only in vertebrate cells that express the enzymes required for the conversion of tryptophan to melatonin, *i.e.* pinealocytes and certain retinal photoreceptors.

The function of scAANAT in yeast requires further consideration. A report in the literature (5) demonstrates that *S. cerevisiae* can produce melatonin when cultured in a standard enriched medium. Furthermore, they can synthesize melatonin from tryptophan, serotonin, or *N*-acetylserotonin when added to cells cultured for a brief time in salt medium. This generation of melatonin from tryptophan indicates that yeast have enzymatic machinery required for melatonin synthesis from tryptophan. A detailed search of the *S. cerevisiae* genomic data base, however, could not identify a homolog of hydroxyindole *O*-methyltransferase, which is the final enzyme in vertebrate melatonin synthesis.[5] Furthermore, a function for melatonin has not been ascribed in yeast, because there is no circadian rhythm in its production. Given that scAANAT has such high K_m values for serotonin and tryptamine, melatonin synthesis may reflect the opportunistic action of otherwise unrelated metabolic enzymes with broad functions (aromatic hydroxylation, decarboxylation, *N*-acetylation, *O*-methylation).

scAANAT might have a much broader capacity than being dedicated exclusively to melatonin synthesis; it might be involved in acetylating many arylalkylamines. This is based in part on the substrate selectively pattern and on the finding that the level of arylalkylamine acetylation is significantly suppressed in scAANAT$^{(-)}$ mutant yeast. One important consequence of arylalkylamine acetylation is that it would prevent conversion of an amine to an aldehyde, which is potentially toxic because of high reactivity and nonselectivity. Arylalkylamines are present in the environment and can also be generated in cells by decarboxylation of aromatic amino acids, *e.g.* tryptamine from tryptophan, phenylethylamine from phenylalanine, and tyramine from tyrosine. Accordingly, it appears reasonable to consider that the primary function of AANAT early in evolution was detoxification, not photochemical transduction.

Comparison of Fungal and Vertebrate AANAT Sequences and Structures—The structural relationship between scAANAT and vertebrate AANATs was investigated by molecular modeling of the yeast sequence to the known structure of oAANAT. The model incorporated 174 of 191 amino acids in scAANAT and supports the hypothesis that scAANAT assumes the same three-dimensional structure as that established for vertebrate AANAT, consistent with the conserved pattern of substrate specificity and sensitivity to the AANAT inhibitor CoA-S-*N*-acetyltryptamine.

Two differences should be noted between the otherwise similar fungal and vertebrate sequences. One is that the regions flanking the catalytic core (residues 28–201; Ref. 33) exhibit essentially no similarity. These flanking regions are not essential for catalysis (12, 33). Rather, it is likely that they are involved in regulation, based on the presence of PKA phosphorylation sites at both the N- and C-terminal flanking regions and evidence that cAMP regulates the abundance of AANAT protein by inhibiting proteasomal proteolysis. cAMP appears to regulate AANAT activity by directing binding to 14-3-3 proteins, through the 14-3-3 binding motif, which encompasses the N-terminal PKA site (29, 30). Proteasomal proteolysis may involve ubiquitination at the conserved lysine in the N-terminal region of vertebrate AANAT. The absence of these flanking

[5] S. L. Coon and D. C. Klein, unpublished observations.

regulatory regions in scAANAT indicates that these regions may have been acquired by AANAT early in vertebrate evolution as the enzyme become involved in photochemical transduction.

A second difference between vertebrate and scAANAT structures occurs in loop 1, a mobile element of the protein that participates in the formation of arylalkylamine binding site. The crystal structures of the free and complexed forms of oAANAT are consistent with a model in which loop 1 moves and undergoes α-helical reorganization during catalysis (28). Comparison of scAANAT and oAANAT structures indicates substantial conservation near the ends of loop 1. However, notable differences exist in the intervening sequence in both the composition and length. Specifically, loop 1 is three residues shorter in scAANAT and lacks a residue corresponding to Pro-64 of oAANAT, which appears to sandwich the aromatic ring of arylalkylamines against oAANAT Phe-188 (scAANAT Phe-172). These differences in loop 1 may explain the lower specific activity of scAANAT, because this flexibility appears to be required to enable substrate/product flux through the active core of the enzyme. Differences in relative affinity for substrates may reflect differences in the composition of loop 1.

Sequence comparison may also provide an explanation for the observation that the optimal pH of scAANAT and oAANAT for tryptamine differ significantly, with scAANAT requiring a higher pH for maximal activity. This may reflect the influence of pH on proton elimination, which would be favored at higher pH value. It is possible that proton elimination is more efficient at pH 7 in the case of vertebrate AANATs, as compared with scAANAT. This difference in pH optima may reflect differences in the amino acid residues involved in binding the water molecules in the networks that facilitate elimination of protons from the catalytic domain.

A "column" of conserved amino acids is revealed in the scAANAT model. The significance of this column may be structural or functional. Although the importance of this column is not clear, the finding that it exits illustrates that three-dimensional homology modeling can provide insights not obvious from two-dimensional sequence analysis.

Other Predicted Fungal AANATs—Evidence that scAANAT is a functional AANAT provided reason to search for other hypothetical AANATs, using both the vertebrate AANAT and scAANAT sequences as the query in BLAST-based data base searches. This identified additional hypothetical AANATs in fungi, but not in the essentially complete *D. melanogaster* or *C. elegans* genomes, nor other eukaryotic sequences available in the data bases.

A consensus fungal AANAT sequence was derived that encompassed 54% (103/191) of the *S. cerevisiae* amino acid residues (Fig. 5). This high degree of conservation across three fungal subphyla is consistent with the view that all fungal AANATs are *bona fide* orthologs and encode functional enzymes.

The absence of AANATs in the nearly complete *D. melanogaster* or *C. elegans* genomes or in any eukaryote other than fungi and vertebrates is difficult to explain. One explanation is that the gene was vertically transmitted through the course of evolution, and was deleted in certain phylogenetic lineages. This may have involved independent losses from *D. melanogaster* and *C. elegans.* However, recent molecular phylogenies suggest that arthropods and nematodes may have derived from a common ancestor (34). If this were true, then a single gene loss event could account for this absence. It is also not impossible that the limited distribution of AANAT may in part reflect lateral transfer, for example, from bacteria to an ancestral fungus and to an ancestral vertebrate.

These studies establish the presence of a functional AANAT in *S. cerevisiae* and raise interesting questions about the evolution of the AANAT family and the function of specific elements of the protein. It is expected that future research may provide answers to some of these questions.

Acknowledgments—We express our appreciation to Dr. Eugene Koonin (NCBI, National Institutes of Health, Bethesda, MD) for helpful discussions regarding sequence analysis and phylogenetic analysis and to Dr. Henry Fales (Laboratory of Biophysical Chemistry, NHLBI, National Institutes of Health, Bethesda, MD) for technical assistance.

REFERENCES

1. Coon, S. L., Roseboon, P. H., Baler, R., Weller, J. L., Namboodiri, M. A. A., Koonin, E. V., and Klein, D. C. (1995) *Science* **270,** 1681–1683
2. Klein, D. C., Coon, S. L., Roseboom, P. H., Weller, J. L., Bernard, M., Gastel, J. A., Zatz, M., Iuvone, M., Rodriquez, I. R., Begay, V., Falcón, J., Cahill, G., Cassone, V. M., and Baler, R. (1997) *Rec. Prog. Horm. Res.* **52,** 307–358
3. Neuwald, A. F., and Landsman, D. (1997) *Trends Biochem. Sci.* **22,** 154–155
4. Dyda, F., Klein, D. C., and Hickman, A. B. (2000) *Annu. Rev. Biophys. Biomol. Struct.* **29,** 81–103
5. Sprenger, J., Hardeland, R., Fuhrberg, B., and Han, S.-J. (1999) *Cytologia* **64,** 209–213
6. Hardeland, R. (1999) *Reprod. Nutr. Dev.* **39,** 399–408
7. Laemmli, U. K. (1970) *Nature* **227,** 680–685
8. Lorenz, M. C., Muir, R. S., Lim, E., McElyer, J., Weber, S. C., and Heitman, J. (1995) *Gene* (*Amst.*) **158,** 113–117
9. Namboodiri, M. A. A., Dubbles, R., and Klein, D. C. (1987) *Methods Enzymol.* **142,** 583–590
10. Riodan, J. F., and Vallee, B. L. (1972) *Methods Enzymol.* **25,** 494–499
11. Khalil, E. M., and Cole, P. A. (1998) *J. Am. Chem. Soc.* **120,** 6195–6196
12. De Angelis, J., Gastel, J., Klein, D. C., and Cole, P. A. (1998) *J. Biol. Chem.* **273,** 3045–3050
13. Altschul, S. F., Madden, T. L., Schaffer, A. A., Zhang, J., Miller, W., and Lipman, D. J. (1997) *Nucleic Acids Res.* **25,** 3389–3402
14. Thompson, J. D., Higgins, D. G., and Gibson, T. J. (1994) *Nucleic Acids Res.* **22,** 4673–4680
15. Levitt, M. (1992) *J. Mol. Biol.* **226,** 507–533
16. Brooks, B. R., Bruccoleri, R. E., Olafson, B. D., States, D. J., Swaminathan, S., and Karplus, M. (1983) *J. Comput. Chem.* **4,** 187–217
17. MacKerell, A. D., Jr., Bashford, D., Bellott, M., Dunbrack, R. L., Jr., Evanseck, J. D., Field, M. J., Fischer, S., Gao, J., Guo, H., Ha, S., Joseph-McCarthy, D., Kuchnir, L., Kuczera, K., Lau, F. T. K., Mattos, C., Michnick, S., Ngo, T., Nguyen, D. T., Prodhom, B., Reiher, W. E., III, Roux, B., Schlenkrich, M., Smith, J. C., Stote, R., Straub, J., Watanabe, M., Wiorkiewicz-Kuczera, J., Yin, D., and Karplus, M. (1998) *J. Phys. Chem. B* **102,** 3586–3616
18. Brunger, A. T., and Karplus, M. (1988) *Proteins Struct. Funct. Genet.* **4,** 148–156
19. Halgren, T. A. (1996) *J. Comput. Chem.* **17,** 490–519
20. Halgren, T. A. (1996) *J. Comput. Chem.* **17,** 520–552
21. Halgren, T. A. (1996) *J. Comput. Chem.* **17,** 553–586
22. Halgren, T. A. (1996) *J. Comput. Chem.* **17,** 587–615
23. Halgren, T. A. (1996) *J. Comput. Chem.* **17,** 616–641
24. Kraulis, P. J. (1991) *J. Appl. Crystallogr.* **24,** 946–950
25. Merritt, E. A., and Bacon, D. J. (1997) *Methods Enzymol.* **277,** 505–524
26. Namboodiri, M. A., Nakai, C., and Klein, D. C. (1979) *J. Neurochem.* **33,** 807–810
27. Benyassi, A., Schwartz, C., Coon, S. L., Klein, D. C., and Falcon, J. (2000) *Neuroreport* **11,** 255–258
28. Hickman, A. B., Namboodiri, M. A. A., Klein, D. C., and Dyda, F. (1999) *Cell* **97,** 361–369
29. Obsil, T., Ghirlando, R., Klein, D. C., Ganguly, S., and Dyda, F. (2001) *Cell* **105,** 257–267
30. Ganguly, S., Gastel, J., Weller, J. L., Schwartz, C., Jaffe, H., Namboodiri, M. A. A., Coon, S. L., Hickman, A. B., Rollag, M., Obsil, T., Beauverger, P., Ferry, G., Boutin, J. A., and Klein, D. C. (2001) *Proc. Natl. Acad. Sci. U. S. A.* **98,** 8083–8088
31. Hintermann, E., Grieder, N. C., Amherd, R., Brodbeck, D., and Meyer, U. A. (1996) *Proc. Natl. Acad. Sci. U. S. A.* **93,** 12315–12320
32. Amherd, R., Hintermann, E., Walz, D., Affolter, M., and Meyer, U. A. (2000) *DNA Cell Biol.* **19,** 697–705
33. Hickman, A. B., Klein, D. C., and Dyda, F. (1999) *Mol. Cell* **3,** 23–32
34. Adoutte, A., Balavoine, G., Lartillot, N., Lespinet, O., Prud'homme, B., and de Rosa, R. (2000) *Proc. Natl. Acad. Sci. U. S. A.* **97,** 4453–4456
35. Klein, D. C., Baler, R., Roseboom, P. H., Weller, J. L., Bernard, M., Gastel, J. A., Zatz, M., Iuvone, P. M., Begay, V., Falcon, J. Cahill, G., Cassone, V. M., and Coon, S. L. (1998) in *Handbook of Behavioral State Control* (Lydic, R., and Baghdoyan, H., eds) Vol. 4, pp. 45–49, CRC Press, Boca Raton, FL
36. Coon, S. L., Weller, J. L., Korf, H. W., Namboodiri, M. A. A., Rollag, M., and Klein, D. C. (2001) *J. Biol. Chem.* **276,** 24097–24107